Effect of a finite-energy spread of the positron beam on the threshold behavior of the positron annihilation cross section

J. Ludlow and G. F. Gribakin
Department of Applied Mathematics and Theoretical Physics, Queen's University, Belfast BT7 1NN, Northern Ireland, United Kingdom
(Received 31 May 2002; published 31 December 2002)

In a recent paper [Phys. Rev. Lett. **88**, 163202 (2002)] we established the threshold behavior of the cross section of positron-atom annihilation into two γ quanta near the positronium (Ps)-formation threshold. Here, the near-threshold behavior of the positron 3γ annihilation cross section and its relation to the ortho-Ps-formation cross section are determined. We also analyze the feasibility of observing these effects by examining the effect of the finite-energy resolution of a positron beam on the threshold behavior.

DOI: 10.1103/PhysRevA.66.064704 PACS number(s): 34.85.+x, 36.10.Dr, 78.70.Bj, 03.65.Nk

Threshold phenomena and threshold laws occupy a special place in atomic, nuclear, and particle physics. In general, they provide an analytical description of cross sections in a near-threshold energy range in many problems [1] which can otherwise only be treated numerically.

In a previous paper [2], we examined the behavior of the two-photon positron annihilation rate near the positronium (Ps) formation threshold in positron-atom collisions. The threshold energy is equal to the ionization potential I less than the ground-state Ps binding energy $|E_{1s}|=6.8$ eV, $\varepsilon_{\rm thr}=I-|E_{1s}|$. It was found that as the positron energy ε approaches the Ps-formation threshold, the annihilation cross section exhibits a characteristic growth $\sigma_{2\gamma}\propto(\varepsilon_{\rm thr}-\varepsilon)^{-1/2}$. This increase is related to the contribution of virtual parapositronium (p-Ps) to the two-photon annihilation. When the finite lifetime of p-Ps was taken into account the near-threshold onset two-photon annihilation cross section was found to be equal to the p-Ps formation cross section.

In this paper we investigate the feasibility of experimental verification of these predictions. Such measurements have become possible due to a recent development of a cold positron beam tunable over a wide energy range [3]. This tool has already provided new data on positron scattering from atoms and molecules [4] and unique information on the role of vibrations in positron-molecule annihilation [5]. However, if this threshold behavior is to be detected experimentally then the finite-energy width of the positron beam ($\sim$20 meV) must be taken into account. This energy spread makes the threshold behavior difficult to detect. At $\varepsilon<\varepsilon_{\rm thr}$, the high-energy "tail" of the positron-energy distribution will overlap the Ps-formation threshold, thus causing the annihilation signal to be swamped by annihilation of "real" Ps.

Annihilation into two γ quanta takes place when the total spin of the electron-positron pair is zero, $S=0$. In the opposite case, $S=1$, the pair annihilates into three γ quanta [6]. In positron-atom collisions with unpolarized particles the rate of 3γ annihilation is about 400 times smaller than that of 2γ annihilation [7], and it is usually neglected at $\varepsilon<\varepsilon_{\rm thr}$. However, at higher energies Ps formation followed by its eventual annihilation becomes the dominant annihilation mechanism. When Ps is formed in positron-atom collisions, the spins of the positron and electron combine statistically, which means that the probability of forming p-Ps ($S=0$) is $\frac{1}{4}$, and that of orthopositronium (o-Ps, $S=1$) is $\frac{3}{4}$. As a result, above the Ps-formation threshold 3γ annihilation takes over the 2γ annihilation. Therefore, to account for the effect of the tail of the positron-energy distribution we first need to examine the threshold behavior of the 3γ annihilation cross section.

Both the two- and three-photon annihilation cross sections are proportional to the density of the positron at each of the target electrons [6],

$$Z_{\rm eff}=\int\sum_{i=1}^{N}\delta(\mathbf{r}_i-\mathbf{r})|\Psi(\mathbf{r}_1,\dots,\mathbf{r}_N,\mathbf{r})|^2 d\mathbf{r}_1\dots d\mathbf{r}_N d\mathbf{r}, \tag{1}$$

where $\Psi(\mathbf{r}_1,\dots,\mathbf{r}_N,\mathbf{r})$ is the full $(N+1)$-particle wave function of the N electron coordinates $\mathbf{r}_i$ and positron coordinate $\mathbf{r}$. The wave function is normalized to a positron plane wave at large distances,

$$\Psi(\mathbf{r}_1,\dots,\mathbf{r}_N,\mathbf{r})\simeq\Phi_0(\mathbf{r}_1,\dots,\mathbf{r}_N)e^{i\mathbf{k}\cdot\mathbf{r}},$$

where $\Phi_0(\mathbf{r}_1,\dots,\mathbf{r}_N)$ is the target ground-state wave function, and $\mathbf{k}$ is the incident positron wave number. In this case $Z_{\rm eff}$ is a dimensionless quantity called the effective number of electrons [8].

In terms of $Z_{\rm eff}$, the two-photon and three-photon annihilation cross sections for positrons on a multielectronic target are (cf. [7])

$$\sigma_{2\gamma}=\pi r_0^2(c/v)Z_{\rm eff}, \tag{2}$$

$$\sigma_{3\gamma}=[4(\pi^2-9)/3]\alpha r_0^2(c/v)Z_{\rm eff}, \tag{3}$$

where $\alpha=e^2/\hbar c\approx1/137$, $r_0=e^2/mc^2$ is the classical electron radius, and v is the positron velocity. In what follows we use atomic units ($\hbar=m=|e|=1$), so that, e.g., $v=k$.

Equation (1) does not contain the spin variables of the particles explicitly, since we assume that the directions of the electron and positron spins in the annihilating pair are random. Alternatively, one needs to insert a projection operator for the total spin of an electron-positron pair, $P_S=\frac{1}{2}-(-1)^S(\frac{1}{4}+\mathbf{s}_i\cdot\mathbf{s})$ [9], where $\mathbf{s}_i$ and $\mathbf{s}$ are the electron- and positron-spin operators, into Eq. (1). This procedure will yield the effective number of electron-positron pairs with a given total spin $Z_{\rm eff}^{(S)}$. It must then be used in Eq. (2) for $S=0$, or Eq. (3) for $S=1$, with additional factors of 4 and 4/3 inserted on the right-hand side, respectively. Of course, averaging over the spin of the incident positron yields $\langle P_S\rangle = \frac{1}{2}-(-1)^S\frac{1}{4}$, followed by $Z_{\rm eff}^{(0)}=Z_{\rm eff}/4$ and $Z_{\rm eff}^{(1)}=3Z_{\rm eff}/4$, thereby recovering the original formulas (1)–(3).

The derivation of a threshold law for the three-photon annihilation is similar to that of the two-photon annihilation [2]. However, in this paper we present an alternative derivation which makes full use of the coordinate form of the wave function near the Ps-formation threshold. When the positron is outside the target, it is given by

$$\Psi(\mathbf{r}_1,\ldots,\mathbf{r}_N,\mathbf{r})\simeq\Phi_0(\mathbf{r}_1,\ldots,\mathbf{r}_N)\left(e^{i\mathbf{k}\cdot\mathbf{r}}+f\frac{e^{ikr}}{r}\right)+\hat{A}\Phi_i(\mathbf{r}_1,\ldots,\mathbf{r}_N)f_{\rm Ps}\frac{e^{iKR}}{R}\varphi_{1s}(\boldsymbol{\rho}), \tag{4}$$

where the second term corresponds to the outgoing Ps formed by the positron and one of the electrons. Here, Φ_i is the wave function of the target ion left after the removal of the ith electron, $\hat{A}$ is the electron antisymmetrization operator, f and $f_{\rm Ps}$ are the elastic scattering and Ps-formation amplitudes, respectively. In the Ps term, $\mathbf{R}=(\mathbf{r}_i+\mathbf{r})/2$ is the Ps center of mass, $\boldsymbol{\rho}=\mathbf{r}_i-\mathbf{r}$ is the internal Ps coordinate, $\varphi_{1s}(\boldsymbol{\rho})=(8\pi)^{-1/2}\exp(-2\rho)$ is the Ps ground state wave function.

In Eq. (4), K is the Ps momentum given by energy conservation,

$$\varepsilon-I=K^2/2M+E_{1s}, \tag{5}$$

as $K=\sqrt{2M(\varepsilon-\varepsilon_{\rm thr})}$, where $M=2$ a.u. is the Ps mass. Below threshold, $\varepsilon<\varepsilon_{\rm thr}$, the Ps momentum is imaginary, $K=i|K|=i2\sqrt{\varepsilon_{\rm thr}-\varepsilon}$, and the corresponding term in the wave function (4) decays exponentially. Close to threshold when $|K|$ is small, the exponent $e^{-|K|R}$ extends over a large range of distances $R\sim|K|^{-1}\gg1$. The contribution of the Ps-formation term becomes dominant in $Z_{\rm eff}$,

$$Z_{\rm eff}\simeq\int\delta(\boldsymbol{\rho})|f_{\rm Ps}|^2e^{-2|K|R}R^{-2}|\varphi_{1s}(\boldsymbol{\rho})|^2d\mathbf{R}d\boldsymbol{\rho}. \tag{6}$$

In accord with the general threshold law theory [9], the Ps formation at threshold is dominated by the Ps s wave, and the amplitude $f_{\rm Ps}$ remains finite and does not depend on the Ps angle of emission. After an elementary integration one obtains,

$$Z_{\rm eff}\simeq\frac{|f_{\rm Ps}|^2}{8\sqrt{\varepsilon_{\rm thr}-\varepsilon}}, \tag{7}$$

which means that both $\sigma_{2\gamma}$ and $\sigma_{3\gamma}$ display a characteristic $(\varepsilon_{\rm thr}-\varepsilon)^{-1/2}$ increase towards the threshold [2].

However, Eq. (7) makes an unphysical prediction that the annihilation cross sections are infinite in the limit $\varepsilon\to\varepsilon_{\rm thr}$. It is also clear that the above approach cannot be applied to calculate the annihilation rate above the Ps-formation threshold, where real Ps formation is the dominant annihilation mechanism. There the momentum K is real and the integral analogous to that in Eq. (6) diverges as $\int dR$.

Both defects are remedied when a finite lifetime of Ps is taken into account [2]. This lifetime is reciprocal to the energy width Γ of the Ps atom, which means that the Ps energy acquires a small imaginary part

$$E_{1s}\to E_{1s}-i\Gamma/2. \tag{8}$$

The widths of p-Ps and o-Ps are determined by the rates of 2γ and 3γ annihilation of $S=0$ and $S=1$ states, respectively [6],

$$\Gamma_p=\frac{r_0^2c}{2},\quad \Gamma_o=\frac{2(\pi^2-9)}{9\pi}\alpha r_0^2c. \tag{9}$$

As a result, the Ps momentum now always has an imaginary part [10],

$$K=\sqrt{2M(\varepsilon-\varepsilon_{\rm thr}+i\Gamma/2)}\equiv K'+iK'', \tag{10}$$

where

$$K'=\sqrt{M}(\sqrt{\Delta\varepsilon^2+\Gamma^2/4}+\Delta\varepsilon)^{1/2}, \tag{11}$$

$$K''=\sqrt{M}(\sqrt{\Delta\varepsilon^2+\Gamma^2/4}-\Delta\varepsilon)^{1/2}, \tag{12}$$

$\Delta\varepsilon=\varepsilon-\varepsilon_{\rm thr}$, and $\Gamma=\Gamma_p$ or Γ_o must be used, depending on whether we consider p-Ps or o-Ps. The real and imaginary parts of K are related through

$$K'K''=M\Gamma/2, \tag{13}$$

and since $K'(\Delta\varepsilon)=K''(-\Delta\varepsilon)$, one also has $K'(\Delta\varepsilon)K'(-\Delta\varepsilon)=M\Gamma/2$, and a similar relation for K''.

Over a narrow energy range $|\Delta\varepsilon|\sim\Gamma$ the real and imaginary parts of K are comparable. This range corresponds to the uncertainty in the position of the threshold introduced by the finite Ps lifetime. Beyond that ($|\Delta\varepsilon|\gg\Gamma$) the real part of K dominates above threshold, while below threshold, K is almost purely imaginary.

Due to a positive K'', the Ps part of the wave function (4) decreases with distance as $\exp(-K''R)$. Below threshold this drop is a consequence of the Ps being virtual, while above threshold the loss of the positron flux is due to annihilation of Ps. Indeed, the Ps density is proportional to $\exp(-2K''R)=\exp(-\Gamma R/V)$, where $V=K'/M$ above threshold is the Ps velocity, and R/V is the time it takes the Ps to reach R. Most importantly, this behavior ensures that the Ps contribution to the integral (1) is now always finite,

$$Z_{\rm eff}\simeq\int\delta(\boldsymbol{\rho})|f_{\rm Ps}|^2e^{-2K''R}R^{-2}|\varphi_{1s}(\boldsymbol{\rho})|^2d\mathbf{R}d\boldsymbol{\rho} \tag{14}$$

$$=\frac{1}{16\pi K''}\int|f_{\rm Ps}|^2d\Omega, \tag{15}$$

the last integral being over the Ps angles of emission. Close to threshold where the Ps is mostly in the s wave, $\int|f_{\rm Ps}|^2d\Omega\simeq4\pi|f_{\rm Ps}|^2$.

Using Eqs. (2), (3), (12), and (14) we immediately obtain expressions for the annihilation cross sections which are valid throughout the near-threshold region,

$$\sigma_{2\gamma} \simeq \frac{\pi r_0^2 c |f_{\mathrm{Ps}}|^2}{8k\left[\frac{1}{2}(\sqrt{\Delta\varepsilon^2+\Gamma_p^2/4}-\Delta\varepsilon)\right]^{1/2}}, \tag{16}$$

$$\sigma_{3\gamma} \simeq \frac{(\pi^2-9) r_0^2 c \alpha |f_{\mathrm{Ps}}|^2}{6k\left[\frac{1}{2}(\sqrt{\Delta\varepsilon^2+\Gamma_o^2/4}-\Delta\varepsilon)\right]^{1/2}}. \tag{17}$$

The first of these is identical to Eq. (21) of Ref. [2], except we used a different amplitude, $A_{\mathrm{Ps}} = -\pi f_{\mathrm{Ps}}$. At energies below threshold and outside the narrow positron-energy-width range, $|\Delta\varepsilon| \gg \Gamma$ (whose size is different for 2γ and 3γ annihilation) one has

$$\sigma_{2\gamma} \simeq \frac{\pi\Gamma_p |f_{\mathrm{Ps}}|^2}{4k\sqrt{\varepsilon_{\mathrm{thr}}-\varepsilon}}, \tag{18}$$

$$\sigma_{3\gamma} \simeq \frac{3\pi\Gamma_o |f_{\mathrm{Ps}}|^2}{4k\sqrt{\varepsilon_{\mathrm{thr}}-\varepsilon}}, \tag{19}$$

with a characteristic $(\varepsilon_{\mathrm{thr}}-\varepsilon)^{-1/2}$ rise towards threshold.

Above threshold at $|\Delta\varepsilon| \gg \Gamma$, Eqs. (16) and (17) become

$$\sigma_{2\gamma} \simeq (\pi/k)\sqrt{\varepsilon-\varepsilon_{\mathrm{thr}}}|f_{\mathrm{Ps}}|^2, \tag{20}$$

$$\sigma_{3\gamma} \simeq (3\pi/k)\sqrt{\varepsilon-\varepsilon_{\mathrm{thr}}}|f_{\mathrm{Ps}}|^2. \tag{21}$$

These cross sections are equal to $\frac{1}{4}$ and $\frac{3}{4}$ of the total Ps-formation cross section,

$$\sigma_{\mathrm{Ps}} = \frac{K}{Mk}\int |f_{\mathrm{Ps}}|^2 d\Omega, \tag{22}$$

which follows from wave function (4), given the fact that $f_{\mathrm{Ps}}=$const near the threshold. Therefore, Eqs. (20) and (21) represent the cross sections for the formation of *p*-Ps and *o*-Ps, which subsequently decay into 2γ and 3γ, respectively. This means that because of the finite Ps lifetime, there is no real distinction between positron-atom annihilation near threshold and Ps formation. From this point of view the equations derived are the particular cases of the problem of a threshold law for creation of an unstable particle considered in Ref. [11].

Of course, positrons can also annihilate with one of the electrons while they are at the target. This is the main annihilation mechanism when the positron energy is far below the threshold. Unlike the Ps contributions considered above, annihilation at the target remains constant as the positron energy approaches the threshold, and its relative role becomes very small above threshold where Ps formation is the main annihilation mechanism.

It is clear that below threshold as well as at $\Delta\varepsilon = 0$, the 2γ annihilation cross section is much greater than $\sigma_{3\gamma}$, whereas above the threshold the probability of 3γ annihilation is three times that of 2γ. This behavior is illustrated in Fig. 1.

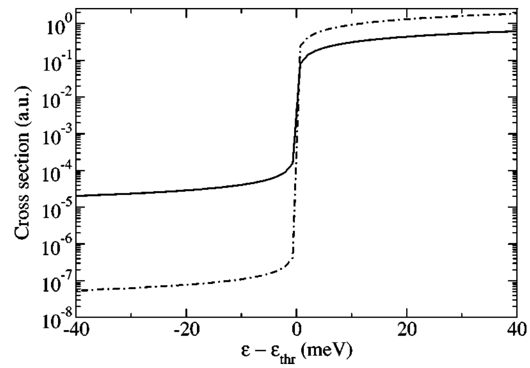

FIG. 1. Two-photon and three-photon annihilation cross sections. The solid curve represents $\sigma_{2\gamma}$ of Eq. (16), and the chain curve is $\sigma_{3\gamma}$ of (17). The cross sections are calculated using $|f_{\mathrm{Ps}}| = 1.78$, an estimate of the Ps formation amplitude for Xe.

In order to detect the threshold behavior of the annihilation cross section experimentally it is important to consider how the energy distribution of the positron beam will affect the threshold behavior. The true energy distribution of the positron beam is not very well known [12]. In this work we approximate it by a Gaussian distribution of the form,

$$f_{\epsilon}(\varepsilon) = \frac{e^{-(\varepsilon-\epsilon)^2/2\delta^2}}{\sqrt{2\pi\delta^2}}, \tag{23}$$

where ϵ is the center of the distribution and δ is the energy width parameter related to the full width at half maximum by $\delta_{\mathrm{FWHM}} = 2\delta\sqrt{2\ln 2}$.

To derive the positron annihilation signal, Eqs. (16) and (17) must now be averaged over the distribution,

$$\overline{\sigma}(\epsilon) = \int \sigma(\varepsilon) f_{\epsilon}(\varepsilon) d\varepsilon. \tag{24}$$

By neglecting the 3γ cross section below threshold, Eq. (21) which describes *o*-Ps formation can then be convolved with the Gaussian to give,

$$\overline{\sigma}_{3\gamma} \simeq \frac{3\pi\sqrt{\delta}|f_{\mathrm{Ps}}|^2}{2\sqrt{2}k} \exp\left[-\frac{(\epsilon-\varepsilon_{\mathrm{thr}})^2}{4\delta^2}\right] D_{-3/2}\left(-\frac{\epsilon-\varepsilon_{\mathrm{thr}}}{\delta}\right), \tag{25}$$

where $D_{-3/2}$ is the parabolic cylinder function [13]. For the 2γ cross section, Eq. (16) must be convolved with the Gaussian numerically.

Apart from the constant contribution of the annihilation at the target, the annihilation signal near the Ps-formation threshold is proportional to the squared Ps-formation amplitude. To put our results on an absolute scale we shall use an estimate of the Ps-formation amplitude for Xe, $|f_{\mathrm{Ps}}| = 1.78$ a.u., inferred from many-body theory calculations [14]. This value is compatible with the result of coupled static calculations of Ps formation for Xe [15]. Among the

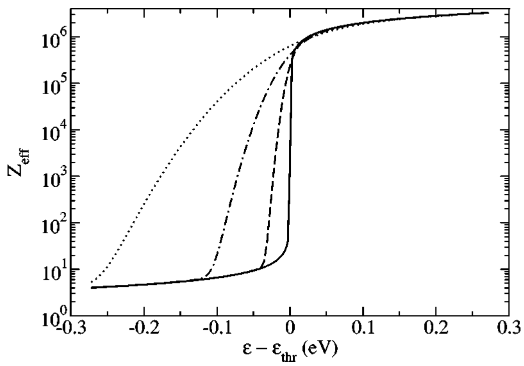

FIG. 2. Total Z_{eff} for Xe as the energy spread of the beam is varied. The solid line is for a monoenergetic beam, the dashed line is 20-meV FWHM, the chain line is 59-meV FWHM, and the dotted line is 139-meV FWHM.

noble gases Xe has the largest Ps-formation cross section (see, e.g., Ref. [16]), and its *s*-wave Ps-formation amplitude is an order of magnitude greater than that for hydrogen [2,17].

The results obtained by adding $\overline{\sigma}_{3\gamma}$ from Eq. (25) to $\overline{\sigma}_{2\gamma}$ calculated numerically from Eqs. (16), (23), and (24), are shown in Fig. 2. The results are given in terms of the quantity Z_{eff}, as used in experiments, via the relation $Z_{\mathrm{eff}} = \sigma_a/[\pi r_0^2(c/v)]$, where $\sigma_a = \overline{\sigma}_{2\gamma} + \overline{\sigma}_{3\gamma}$ is the annihilation cross section.

The cross sections in Fig. 2 correspond to $\delta_{\mathrm{FWHM}} = 20$, 59, and 139 meV. Presently, positron beams with an energy resolution of about 20 meV are available. As is clear from the figure, a major increase in beam resolution will be needed in order to see the near-threshold enhancement predicted by Eq. (18). However, if the energy distribution of the beam is accurately known it may be possible to measure the near-threshold annihilation in order to extract the value of $|f_{\mathrm{Ps}}|$. Alternatively, one may use the known shape of the annihilation cross section near threshold, Eqs. (16) and (17), to analyze the positron energy distribution in the beam.

In conclusion, the behavior of the 3γ annihilation cross section has been determined near the Ps-formation threshold. It is equal to the *o*-Ps-formation cross section in the threshold region. Using these results together with previous results obtained for the 2γ annihilation cross section we have modeled the effect of a finite energy width on threshold behavior. We have found that detecting the threshold behavior of the positron annihilation cross section experimentally will be very challenging.

The method we used to derive the annihilation cross section is based on the standard expression for the annihilation parameter Z_{eff}, Eq. (1). It is applicable at all positron energies including those above threshold, where annihilation is dominated by positronium formation. This also allows one to calculate the annihilation cross section precisely for targets with $I < 6.8$ eV, where Ps formation is open at all energies.

Note added in proof. We would like to thank I. Shimamura for pointing out to us that the *o*-Ps formation threshold lies 0.84 meV above that of *p*-Ps (see, e.g., [6]). We have neglected this small effect in the present study.

We would like to thank C. M. Surko for useful discussions, and H. R. J. Walters and M. T. McAlinden for providing their Ps-formation data. The work of J.L. has been supported by DEL.

[1] E.P. Wigner, Phys. Rev. **73**, 1002 (1948); G.H. Wannier, *ibid.* **90**, 817 (1953); A.I. Baz', Zh. Exp. Teor. Fiz. **33**, 923 (1957) [Sov. Phys. JETP **6**, 709 (1958)]; G. Breit, Phys. Rev. **107**, 1612 (1958).

[2] G.F. Gribakin and J. Ludlow, Phys. Rev. Lett. **88**, 163202 (2002).

[3] S.J. Gilbert, C. Kurz, R.G. Greaves, and C.M. Surko, Appl. Phys. Lett. **70**, 1944 (1997).

[4] S.J. Gilbert, R.G. Greaves, and C.M. Surko, Phys. Rev. Lett. **82**, 5032 (1999); J.P. Sullivan, S.J. Gilbert, and C.M. Surko, *ibid.* **86**, 1494 (2001); J.P. Sullivan, J.P. Marler, S.J. Gilbert, S.J. Buckman, and C.M. Surko, *ibid.* **87**, 073201 (2001).

[5] S.J. Gilbert, L.D. Barnes, J.P. Sullivan, and C.M. Surko, Phys. Rev. Lett. **88**, 043201 (2002); J.P. Sullivan, S.J. Gilbert, J.P. Marler, L.D. Barnes, S.J. Buckman, and C.M. Surko, Nucl. Instrum. Methods Phys. Res. B **192**, 3 (2002).

[6] V.B. Berestetskii, E.M. Lifshitz, and L.P. Pitaevskii, *Quantum Electrodynamics* (Pergamon, Oxford, 1982).

[7] This ratio is determined by the spin-averaged nonrelativistic cross sections of two-photon and three-photon electron-positron annihilation, $\sigma_{2\gamma} = \pi r_0^2 c/v$ and $\sigma_{3\gamma} = [4(\pi^2 - 9)/3]\alpha r_0^2(c/v)$, where $\alpha = e^2/\hbar c \approx 1/137$, r_0 is the classical electron radius, and v is the relative velocity, Ref. [6].

[8] P.A. Fraser, Adv. At. Mol. Phys. **4**, 63 (1968).

[9] L.D. Landau and E.M. Lifshitz, *Quantum Mechanics*, 3rd ed. (Pergamon, Oxford, 1977).

[10] This point [together with Eq. (13)] is used in the analysis of A. Igarashi, M. Kimura, and I. Shimamura, Phys. Rev. Lett. **89**, 123201 (2002), published after the submission of the present paper. However, their conclusion about the breakdown of Eq. (1) near the Ps-formation threshold is incorrect, and the analytical expression (16) derived from Eq. (1) is in perfect agreement with their numerical results close to threshold.

[11] A.I. Baz, Zh. Eksp. Teor. Fiz. **40**, 1511 (1961) [Sov. Phys. JETP **13**, 1058 (1961)].

[12] C.M. Surko (private communication).

[13] I.S. Gradshteyn and I.M. Ryzhik, *Tables of Integrals, Series and Products* (Academic Press, London, 1980).

[14] G.F. Gribakin (unpublished).

[15] M.T. McAlinden and H.R.J. Walters, Hyperfine Interact. **89**, 407 (1994); H.R.J. Walters (private communication).

[16] G. Laricchia, P. Van Reeth, M. Szłuińska, and J. Moxom, J. Phys. B **35**, 2525 (2002).

[17] P. Van Reeth and J.W. Humberston, J. Phys. B **28**, L511 (1995); J.W. Humberston, P. Van Reeth, M.S.T. Watts, and W.E. Meyerhof, *ibid.* **30**, 2477 (1997).